ACS EARTH AND SPACE CHEMISTRY

http://pubs.acs.org/journal/aesccq

Article

Short-Term Soil CO_2 Concentration Responses to Precipitation Events in Karst Land with Diverse Vegetation Coverage in Southwestern China

Yucong Fu,* Jie Zeng, and Zhongjun Wang

Cite This: *ACS Earth Space Chem.* 2023, 7, 2062–2072

Read Online

ACCESS | Metrics & More | Article Recommendations

ABSTRACT: Exploring the short-term fluctuations in soil carbon dioxide (CO_2) concentrations is critical for understanding the terrestrial carbon (C) cycle, especially in karst soil due to its vast C reserves and fragile eco-environment. In this study, we investigated the rainfall-event-driven CO_2 concentration variations in the soil profiles of cropland (CR), abandoned cropland (AC), grassland (SG), and secondary forest (SF) in a typical karst watershed by a sensor technique to understand the short-term soil CO_2 dynamics and their controls at different recovery stages. Our results showed that the CO_2 concentrations in all studied soil types responded to rainfall quickly and decreased significantly during rainfall. CR had the largest decrease (1350 ppm), followed by AC (912 ppm), with a response time of approximately 150 min. By contrast, the decreases in soil CO_2 in SG and SF were smaller, with decreases of 428 and 155 ppm and shorter response times of approximately 45 min. The soil CO_2 concentration showed an obvious diurnal variation pattern consistent with the soil temperature, but there was a lag effect of soil CO_2. After rainfall, the diurnal difference in soil CO_2 concentration decreased, which may be due to a decrease in temperature difference or may be related to soil CO_2 entering groundwater or being consumed by the chemical weathering of carbonates. Our data indicated that the sensitivity of both soil C production and loss to environmental changes such as temperature and precipitation varies in soils with different vegetation recoveries in karst areas. As vegetation recovers, CO_2 drops less during rainfall, suggesting that vegetation recovery enhances soil C stability, thereby helping to sequester atmospheric CO_2 and contribute to the enhancement of C sink functions in karst ecosystems.

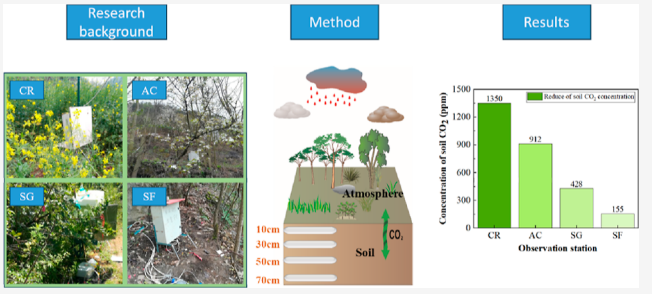

KEYWORDS: *karst, rainfall, soil CO_2, soil temperature, soil moisture content*

1. INTRODUCTION

The increasing concentration of anthropogenic CO_2 in Earth's atmosphere has been closely monitored in the last few decades.[1] Numerous studies suggested that Earth will experience a series of global environmental changes (including frequent droughts and floods in some areas with large population) if continuing on this trend, which greatly threatens sustainable human development.[2] However, the carbon (C) sinks (particularly terrestrial carbon sinks), are still poorly understood, and there is still imbalance between sources and sinks in global C budget.[3,4]

Soil is one of the largest C pools in terrestrial ecosystems.[5,6] Soil CO_2 is a significant contributor to atmospheric CO_2 because it can be emitted into the atmosphere along the concentration gradient.[7,8] On vegetated land, plants thrive in the upper layers of soil and possess the capability of converting inorganic C into organic C through photosynthesis.[9] Upon decomposition, these plants undergo biodegradation and thus transformation into both solid and gaseous components of the soil. The respiration of animals and plants within the soil leads to a higher concentration of CO_2. Soil CO_2 can also be produced by the dissolution of carbonates in calcareous soils.[10] Only at a few exceptional sites is CO_2 derived from geothermal sources.[11] Soil CO_2 can be consumed by the dissolution of minerals in soil and the underlying carbonate rocks,[12] it can also enter rivers via soil pore water when some soil CO_2 is released into the atmosphere,[7] while the rest may be converted into dissolved inorganic C (DIC) in the water body by microorganisms, forming C sinks in a short period of time.[12] In any case, the concentration of soil CO_2 is determined by its production and loss, both of which are subject to various

Received: June 20, 2023
Revised: September 3, 2023
Accepted: September 5, 2023
Published: September 18, 2023

https://doi.org/10.1021/acsearthspacechem.3c00169
ACS Earth Space Chem. 2023, 7, 2062–2072

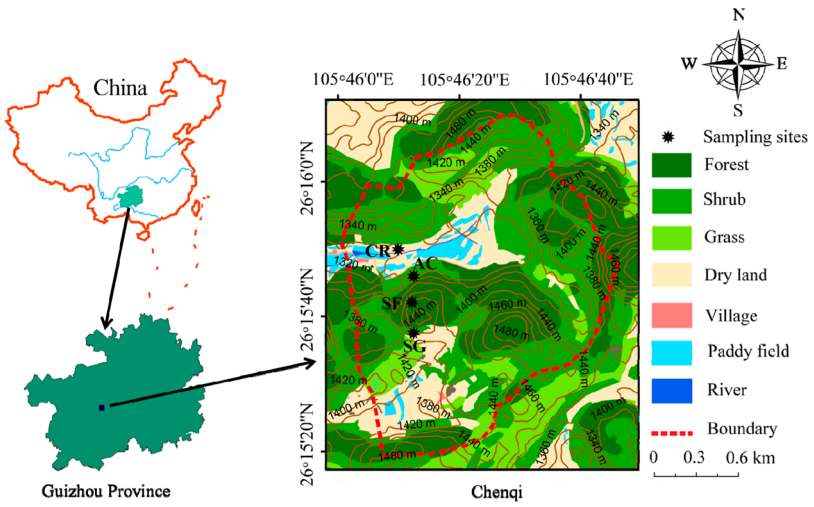

Figure 1. Location and land use of the Chenqi catchment (modified from Wang et al.[31]).

factors, including soil temperature, moisture, and organic matter content.

Many efforts have been made to understand soil CO_2 dynamics in different types of vegetated lands. For instance, Flechard et al.[13] conducted long-term monitoring of grassland soil to quantify the time-dependent changes in soil CO_2 storage, showing that atmospheric turbulence on a diurnal scale has a dynamic impact on CO_2 storage in soil and that diurnal variations in CO_2 concentrations are significantly correlated with soil temperature.[14] The studies on forest systems showed that temperature can promote CO_2 production and change diffusion coefficient.[15] Huang et al.[16] studied the concentration of soil CO_2 in arid areas, suggesting that the daily time scale is mainly affected by temperature, and the soil moisture content is the main limiting factor on the annual scale. During the humid season, the moisture content and its pulse effect may become the key driving factors affecting the dynamics of soil CO_2.[14,17] Even a small amount of rainfall could significantly affect soil C dynamics by triggering the activity of biological crusts,[18] and the impact of soil moisture on soil CO_2 after rainfall was underestimated.[19] During a rainfall event, a large amount of material migrates from the soil to the river and lake system. In this process, there is a common understanding that a large part of river DIC comes from soil CO_2,[20−22] which has a significant impact on C storage and migration in aquatic systems. However, the effect of rainfall on soil C dynamics is still unclear, which limits our understanding of the dynamics of soil C on the river DIC content. Moreover, in alkaline soils, a recent study found a negative flux of soil CO_2 in extreme cases, indicating that the absorption of CO_2 is so pronounced.[10] Carbonate rock is widely involved in karstification and biological processes in karst areas, which have a significant impact on the global C cycle as a result of interaction among water, rock, soil, atmosphere, and biological processes.[23,24] Therefore, it is essential to understand the dynamics of soil CO_2 in karst areas.

However, most of previous studies focused on respiration in surface soils, which may neglect information at deeper depths.[19] Recently, industrial solid-state sensors were developed to enable continuous and in situ monitoring of soil CO_2 profiles.[14,15,25] The development of new CO_2 sensor techniques has facilitated high-frequency measurements, making investigations into hourly and subhourly changes in soil CO_2 concentrations possible.[26,27] Rey et al.[28] highlighted the potential of these new technologies (including advanced automatic chambers, CO_2 concentration profiles, and isotope techniques) in providing further insights into the dynamics and sources of C in the soil.

This study employed an infrared probe, which is in conjunction with temperature and water content probes, to monitor the soil CO_2 concentration, temperature, and moisture content in limestone soil profiles with four major vegetation types in the karst regions of southwestern China. Our study is designed to understand the changes of soil CO_2 concentrations during rainfall events in different stages of vegetation restoration and their controlling factors.

2. STUDY AREAS

The Chenqi watershed (26°15′20″−26°16′9″N, 105°46′3″−105°46′50″E), a small agricultural karstic watershed located covering an area of 1.25 km^2, lies in the headwaters of the Houzhai River, Puding County, Guizhou Province, China (Figure 1). Notably, the region is in the center of the Southeast Asian Karst Region. The climate in this region is classified as a subtropical monsoonal climate, and the annual precipitation is primarily concentrated in the summer and autumn, representing more than 80% of the yearly rainfall.[29] During the rainy season of 2017, the accumulated precipitation was approximately 970 mm, amounting to 85.9% of the aggregate annual rainfall, and the mean temperature was 21.3 °C. In contrast, the mean temperature recorded during the arid period was 11.2 °C.[30,31]

The Chenqi catchment represents a typical karst terrain distinguished by peak-cluster depression. Carbonate rocks are extensively distributed throughout this area. The soil profile is shallow and discontinuous, whereas the arable stratum attains a great thickness (>100 cm) in the gentle topography or incline. The area is encircled by star-shaped conical hills, with elevations ranging from 1310 to 1514 m.[32] The main land use types in this catchment are shrubs, grass, forest, and abandoned cropland (AC), which together account for approximately 83% of the total land area. The bottom of the valley is arable land, which accounts for approximately 17% of the landmass, of which 14% is dry land and 3% is paddy fields.[33]

https://doi.org/10.1021/acsearthspacechem.3c00169
ACS Earth Space Chem. 2023, 7, 2062−2072

3. METHODOLOGY

The research involves deploying observation stations at different depths of the soil profile across four distinct types of vegetation cover [cropland (CR), AC, shrub and grassland (SG), and second forest (SF)]. To measure the soil CO_2 concentration, a closed system previously developed to measure the CO_2 concentration in water was used.[34] The system consisted of an NDIR probe (CARBOCAP GMP252, Vaisala, Vantaa, Finland) for the CO_2 concentration in the air, and a gas-permeable pipe was built (Figure 2); the air was

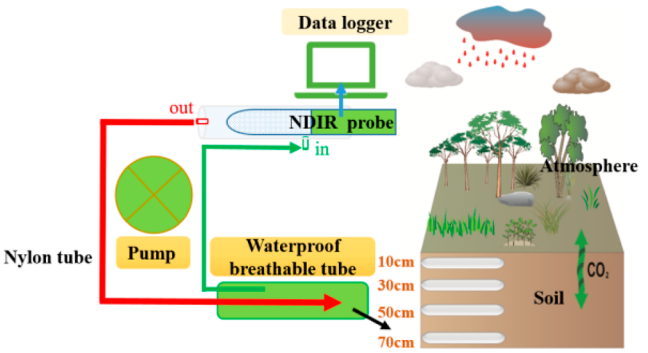

Figure 2. Schematic diagram of the online observation device for the soil CO_2 concentration.

circulated continuously in the system by a diaphragm pump. Since the pipe was designed to have excellent permeability to CO_2, the concentration of CO_2 in the air circulating in the system equilibrated with that in the soil around the tube. The soil CO_2 concentration was measured by installing the gas-permeable pipe horizontally at depths of 10, 30, 50, and 70 cm (Figure 2). A needle-shaped soil temperature and humidity probe (MS10A, China) was deployed to measure the soil temperature and moisture content at the same depth as the CO_2 concentration measurement. Analog voltage outputs of the temperature/humidity and CO_2 concentration probes were used, logged with a data logger, with intervals of 15 min. The system was operated continuously from January 2017, and we reported data from May 3 to 8, 2017. Soils were pulverized and passed through an 80-mesh sieve, acidified with HCl (0.5 mol L^{-1}) for 24 h to remove inorganic C, washed to neutrality using distilled water, dried at 60 °C to a constant weight, and then pulverized and passed through a 100-mesh sieve. Subsamples were used to measure SOC concentrations with an elemental analyzer (Vario MAX CNS analyzer, Elementar Analysensysteme, Hanau, Germany), and data on organic matter have been published in.[30]

On the evening of May 5, 2017, a concentrated rainfall event occurred, resulting in a total rainfall of 18.4 mm. The subsequent dynamics of the soil CO_2 concentration, soil temperature, and soil moisture throughout the profile were observed during the rainfall process.

4. RESULTS

4.1. Soil Temperature and Moisture Content. Prior to precipitation, the soil temperature gradually diminished from the surface layer to the deep layer, aligning with the distribution law of the temperature (Table 2). Before the rain events, in the CR, the soil temperature decreased gradually from the surface layer at 0 cm to the deep layer at 70 cm, and the average temperatures were 22.3, 21.4, 20.4, and 18.5 °C, respectively (Table 2). The surface soil temperature experienced the most significant fluctuation range within the profile, with the range decreasing as the depth increased, and the fluctuation ranges from the surface to deep layer were 9.9, 1.5, 0.9, and 0.5 °C, respectively. Other profiles were slightly different from the specific values of CR, but the trend was consistent. The peak of the diurnal temperature curve of the soil surface appeared at approximately 15:00, and the peak time was delayed relative to the surface layer in deeper soil layers. Below 50 cm, no obvious diurnal variation could be observed. During precipitation, the soil temperature declined dramatically within a short period of time (Figure 3). The surface soil temperature had a significant decrease, while the degree of variation decreased with increasing soil depth, and the ranges from top to bottom were 3.8, 1.1, 0.1, and 0.0 °C. After rainfall, except for 10 cm, there was no obvious diurnal change in the other layers, and the temperature decreased continuously.

Table 1. Site Information on Different Vegetation Types[a]

	pH	SOC g/kg	soil bulk density (g/cm^3)	soil porosity (%)	saturated soil moisture content (cm^3 cm^{-3})	wilting points (cm^3 cm^{-3})
CR-10 cm	6.76	25.79	1.45	0.45	0.43	0.10
CR-30 cm	6.47	19.11	1.54	0.42		
CR-50 cm	6.24	13.28	1.53	0.42		
CR-70 cm	5.73	7.79	1.45	0.45		
AC-10 cm	7.10	34.74	1.29	0.51	0.50	0.10
AC-30 cm	6.38	31.56	1.21	0.55		
AC-50 cm	6.71	19.23	1.29	0.51		
AC-70 cm	6.99	8.08	1.41	0.47		
SG-10 cm	7.29	35.00	1.12	0.58	0.57	0.14
SG-30 cm	6.93	14.64	1.34	0.49		
SG-50 cm	7.07	6.99	1.50	0.43		
SG-70 cm	7.16	8.49	1.47	0.45		
SF-10 cm	5.72	43.42	1.04	0.61	0.57	0.14
SF-30 cm	6.39	25.57	1.29	0.51		
SF-50 cm	6.47	14.10	1.32	0.50		
SF-70 cm	6.27	11.89	1.29	0.51		

[a]Soil pH, SOC, soil bulk density, and soil porosity are from ref 29, and saturated soil moisture content and wilting points are from ref 54.

https://doi.org/10.1021/acsearthspacechem.3c00169
ACS Earth Space Chem. 2023, 7, 2062−2072

Table 2. Average Data of Soil CO_2 Concentration, Temperature, and Moisture Content before, during, and after Rainfall

	soil CO_2 concentration ppm[a]	temperature °C[a]	moisture %[a]	soil CO_2 concentration ppm[b]	temperature °C[b]	moisture %[b]	soil CO_2 concentration ppm[c]	temperature °C[c]	moisture %[c]
CR-10 cm	1132	22.3	16.0	1065	19.0	25.8	1241	17.7	25.1
CR-30 cm	2135	21.4	31.5	1482	21.3	34.3	1188	19.0	35.3
CR-50 cm	5164	20.4	33.9	4324	20.5	34.9	3027	19.4	36.0
CR-70 cm	2094	18.5	37.3	1738	19.0	37.4	1532	18.8	37.6
AC-10 cm	1364	22.0	31.1	1925	16.6	35.0	836	17.8	35.0
AC-30 cm	748	20.8	51.0	875	18.6	54.4	806	18.5	50.2
AC-50 cm	991	19.4	76.3	1077	18.5	86.5	1055	18.7	83.4
AC-70 cm	3266	17.5	63.8	2003	17.3	78.0	2075	17.7	72.0
SG-10 cm	960	20.5	34.4	808	17.5	40.4	848	17.4	36.0
SG-30 cm	667	19.6	63.8	748	18.7	67.6	694	18.0	62.1
SG-50 cm	3348	18.6	62.3	3324	17.3	83.1	2783	18.1	65.0
SG-70 cm	731	17.9	53.3	762	17.3	64.8	690	17.9	59.5
SF-10 cm	1004	18.4	38.5	990	16.7	49.1	1205	16.1	34.0
SF-30 cm	2739	19.2	17.2	2288	18.4	37.2	2700	17.2	35.9
SF-50 cm	719	17.0	38.9	732	17.0	42.4	734	16.5	41.0
SF-70 cm	4519	16.2	26.5	4844	16.4	26.2	4901	16.3	27.0

[a]Represents data obtained prior to rainfall. [b]Represents rainfall data. [c]Represents data after rainfall.

The soil moisture content showed an increasing trend from the surface toward the deep layer (Table 2). Dynamic diurnal fluctuations in the soil moisture content had an apparent pattern at the surface layer, characterized by a low moisture content during the daytime and high moisture at night. However, the degree of diurnal variation weakened with increasing depth and became almost imperceptible at a depth of 70 cm (Figure 3). During precipitation events, the soil moisture content had a rapid and substantial increase with the greatest variation occurring at the surface layer. The increasing rate of moisture content in the CR profile decreased from the surface to the deep layer with increasing rates of 12.9, 3.4, 1.4, and 0.1%, respectively. Taking the CR as an example, within half an hour, the moisture at 10 cm surged from 14.4 to 27.3%, while at 30 cm, it only increased from 31.4 to 34.9%. The soil moisture content at 50 cm appeared to be minimally impacted by the rainfall event. Except for the 10 cm depth at SF, the soil moisture of all of the other sites increased synchronously with rainfall.

4.2. Variation of Soil CO_2 Concentration. There was substantial temporal and spatial variation in soil CO_2 concentrations, with an increase during summer and a decrease during winter.[26,35] In terms of diurnal variation, the CO_2 concentration was typically high during the daytime and low at night. Typically, the concentration of CO_2 increased with depth; however, it exhibited a sharp decline beyond a certain depth (Figure 3). Due to the consumption of soil CO_2 by carbonate dissolution, the soil CO_2 concentration in karst areas often shows a bidirectional gradient in the vertical direction; that is, the maximum soil CO_2 concentration appears in the middle of the soil rather than that at the bottom of the soil.[36] Studies have shown that in the wet season in karst areas, the CO_2 concentration in the bottom soil decreased significantly with increasing depth due to enhanced CO_2 dissolution and the consumption of the bedrock in the limestone soil after rain. During the whole study period, the overall CO_2 concentrations were higher in the SF and CR systems, with concentrations of 2281 and 2177 ppm, respectively, and lower in the AC and SG systems, with concentrations of 1418 and 1364 ppm, respectively.

During rainfall, soil CO_2 undergoes intense fluctuations, wherein it rapidly decreases during intense rainfall and subsequently returns to normal concentration levels in the following days (Figure 3). However, at individual layers of the soil profile, the concentration of CO_2 increased briefly and then decreased rapidly to a low concentration (Figure 3). After rainfall, the diurnal change in the CO_2 concentration was weakened. The diurnal variation in the CO_2 concentration in the soil profiles observed in this study was obvious. Before rainfall, the diurnal variation ranges of the average CO_2 concentration in CR, AC, SG, and SF were 2651, 348, 265, and 236 ppm, respectively. The diurnal variation decreased after rainfall, and the diurnal difference of the four soils decreased to 226, 163, 123, and 142 ppm, respectively. Because the 70 cm depth of the soil belongs to the soil−rock interface, the short-term rainfall process had little influence on this horizon. Therefore, the data of this horizon are not employed in calculating the response amplitudes and times of rainfall. Taking into account the different vegetation types, the average reduction in the CO_2 concentration at CR, AC, SG, and SF was 1350, 912, 428, and 155 ppm, respectively. The response time of CR and AC was approximately 150 min, whereas that of SG and SF with the restoration of vegetation, the soil profile of SG and SF was approximately 45 min.

5. DISCUSSION

During the observation period, the soil CO_2 concentration displayed a rapid decrease when rainfall occurred, followed by a rapid recovery or a slight increase above the prerain level, exhibiting a "V" shaped rapid response pattern. Previous studies on soil CO_2 concentrations indicated an increase in CO_2 concentrations from the surface to deep layers,[15,37] while some studies showed that CO_2 concentrations initially increased and then decreased from the surface to deep layers over time.[36,38] In previous studies, the concentration of soil CO_2 increased with an increase of depth generally. The observed results in the karst area show that this law is not strictly followed and may be related to the special lithology of this area because the carbonate rocks are widely distributed in this area and have discontinuous characteristics. Under the influence of different moisture, temperature, and root

https://doi.org/10.1021/acsearthspacechem.3c00169
ACS Earth Space Chem. 2023, 7, 2062−2072

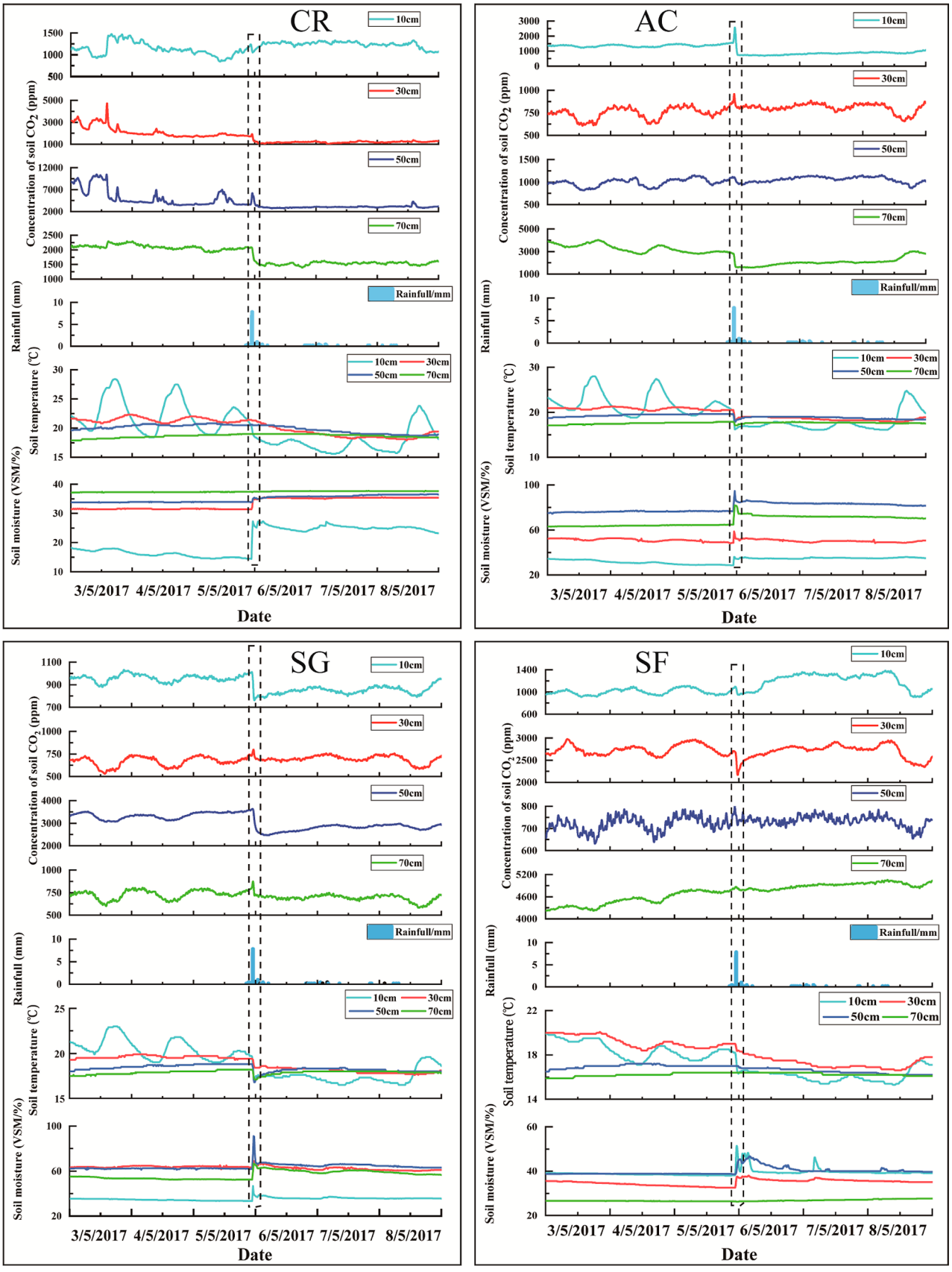

Figure 3. Dynamics in CO_2, soil temperature, and soil moisture content at different depths of CR, AC, SG, and SF profiles during rainfall.

respiration, there will be an imbalance between the production and consumption of soil CO_2 at the same depth, resulting in great differences in the soil CO_2 concentration at different depths. The CR soil profile exhibited an increasing trend of the

https://doi.org/10.1021/acsearthspacechem.3c00169
ACS Earth Space Chem. 2023, 7, 2062−2072

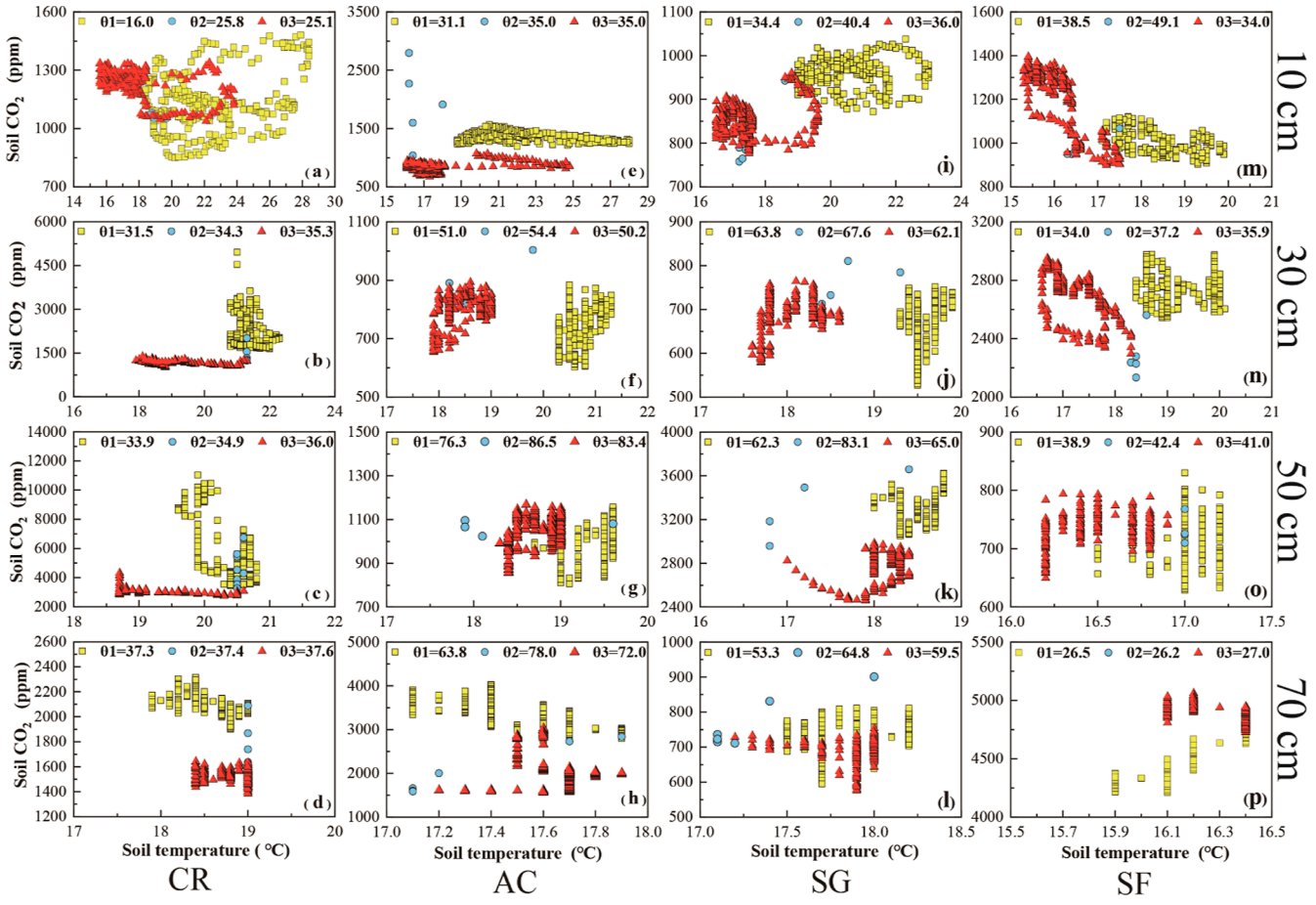

Figure 4. Changes in soil CO_2 and temperature before, during, and after rainfall under different land uses and the influence of the moisture content at different times (θ1, θ2, and θ3 represent the average soil moisture content before, during, and after rainfall, respectively).

CO_2 concentration from the surface layer to a depth of 50 cm and then a decrease. This study initially explored the changes in soil CO_2 concentration under rainfall in different stages of vegetation restoration and the effects of the soil temperature and humidity on the dynamics of CO_2.

5.1. Effects of Vegetation Recovery on Soil CO_2 Changes. The relationship between the soil CO_2 concentration and temperature and moisture content was plotted before and after rainfall (Figures 4 and 6). Overall, the average soil CO_2 concentration before rainfall was higher than that after rainfall. At the four observed points, only the soil CO_2 concentration under SF was higher after rainfall than that before rainfall, which may be caused by the developed root system inherent to the forest. In addition, among the soil under the four vegetation use types, the soil with the least anthropogenic disturbance had a lower level of CO_2 reduction during rainfall. The process of soil conversion from CR to SF or SG was conducive to C fixation and thus reduced C loss.[30] At a depth of 10 cm in the CR, the CO_2 concentration after rain (1241 ppm) was higher than that before rainfall (1132 ppm), which may be due to the respiration restriction of roots and microorganisms by the low soil moisture content of 16.0% prior to the rain. The average moisture content increased from 16.0% before rain to 25.1% after rainfall, which meant that the soil moisture content was no longer a limiting factor, thus leading to an increase in the CO_2 concentration. Below 10 cm of the CR soil, the CO_2 concentration after rainfall was lower than that before rain. A possible reason is that the increase in the moisture content caused the water−rock reaction, which then consumed CO_2 in the soil. On the other hand, the root system of CR soil was shallow, and the CO_2 generation rate of the soil at a deep depth was low, so it was difficult to effectively supplement CO_2. At depths of 30 and 50 cm in the AC, the CO_2 concentration after rainfall was slightly higher than that before rainfall, although the difference was not significant. The reason for the increase after rain may be that pear trees in the AC have deeper root systems, which are conducive to respiration. At 10 and 70 cm, the concentration of CO_2 decreased after rain. As shallow soil was close to the surface in the AC, the addition of water during rain caused CO_2 to enter the atmosphere or move downward into the deep soil. The 70 cm position of the AC was the soil−rock interface, where lateral migration of the soil solution could occur.[39] Furthermore, sufficient water−rock reactions could occur at this horizon, resulting in a large amount of CO_2 consumption.[36,40]

The changes in the soil CO_2 concentration in SF were significantly different from those in other vegetation utilization types. Only at a depth of 30 cm was the CO_2 concentration before rainfall at 2739 ppm greater than that after rainfall (2700 ppm), with a range rate of <5%, this may be related to the effect of the water content on the microbial activity level.[41] In previous studies, it was found that better vegetation restoration could contribute to a higher soil organic C content,[30] which can effectively buffer the C dynamics caused by rainfall. In this study, the diurnal variation of soil CO_2

https://doi.org/10.1021/acsearthspacechem.3c00169
ACS Earth Space Chem. 2023, 7, 2062−2072

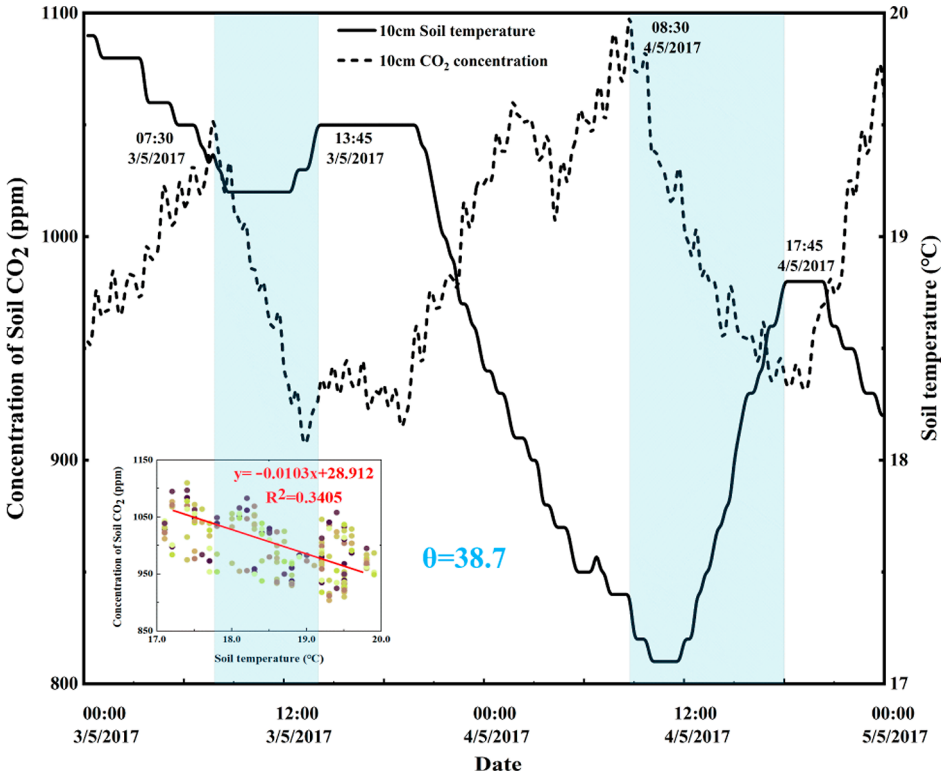

Figure 5. Difference between the soil CO_2 concentration and soil temperature over time. The figure in the lower left corner is the correlation expression of the relationship between soil CO_2 concentration and soil temperature (the average soil moisture content during the period was θ = 38.7).

before and after rainfall decreased with restoration of vegetation (Table 2). After rainfall, with the restoration of vegetation, the resilience of the soil CO_2 concentration is strengthened. According to the data of Table 2, it is found that the CR/AC/SG/SF of soil CO_2 concentration after rain reaches 66, 75, 88, and 106% of that before rainfall, respectively. This shows that with the restoration of vegetation, the root system of vegetation is gradually developed, which is conducive to accelerating the production of CO_2 to supplement the loss of CO_2 during rainfall. In addition, during rainfall, the decrease in the CO_2 concentration decreases with the restoration of vegetation. Although this result may be affected by other factors, according to the observed results, the difference in vegetation cover significantly affects the diurnal variation of soil CO_2 concentration and the performance of the soil CO_2 concentration in the process of rainfall. From the topographic position, SG and SF are close to the top of the slope, and AC and CR are close to the bottom of the valley. The closer the soil is to the outlet of the watershed at the valley bottom, the longer it takes for the soil solution to gather (Figure 1), resulting in a more effective water−rock reaction and a consequent increase in soil CO_2 consumption. Therefore, soil located at the SF with a high organic matter content has the lowest reduction in soil CO_2 during rainfall. In addition, related studies have shown that photosynthesis and soil respiration can be delayed and that a part of soil CO_2 comes from canopy C supply to soil respiration.[42]

5.2. Impact of Soil Temperature on Soil CO_2 Variability. Soil temperature is one of the main factors affecting soil CO_2 concentration,[15,43] which is directly related to the decomposition rate of organic matter and the microbial activity in the soil. Before rainfall, the diurnal variation in soil temperature at the 50 cm and above layers is obvious. After rainfall, the soil temperature in other layers decreased continuously in the following days, except for the surface layer (Figure 3). This change is similar to the concentration of soil CO_2, which decreased continuously after rainfall (Figure 4). Therefore, with the decrease in the diurnal temperature difference of soil temperature after rain, the diurnal variation range of soil CO_2 concentration was also remarkably reduced. The changes in the soil temperature and the CO_2 concentration were not simultaneous (Figure 5). Moreover, there were certain differences between each layer. The surface temperature and CO_2 concentration reach their maximum values on the day before the deep layers. The degree of hysteresis of soil temperature and CO_2 concentration was related to other environmental factors, such as soil moisture (Figure 4). In the rainfall event, the soil temperature is positively related to the CO_2 concentration. When rainfall occurred, both the soil temperature and CO_2 concentrations decreased synchronously throughout different depths and profiles. Previous studies exhibited a positive correlation between soil temperature and CO_2 concentration;[44,45] However, inconsistent results were observed in this study, which may be due to the interference of the rainfall process. Figure 5 shows the large difference between the soil CO_2 concentration and temperature in the 10 cm soil surface layer of the CR when the daily maximum CO_2 concentration was observed and the soil temperature reached the daily maximum in the following afternoon (average moisture during this period θ = 38.7%).

After the lowest value reached in the afternoon, the concentration of CO_2 began to rise and reached the highest value the next morning. The soil temperature at the surface

https://doi.org/10.1021/acsearthspacechem.3c00169
ACS Earth Space Chem. 2023, 7, 2062−2072

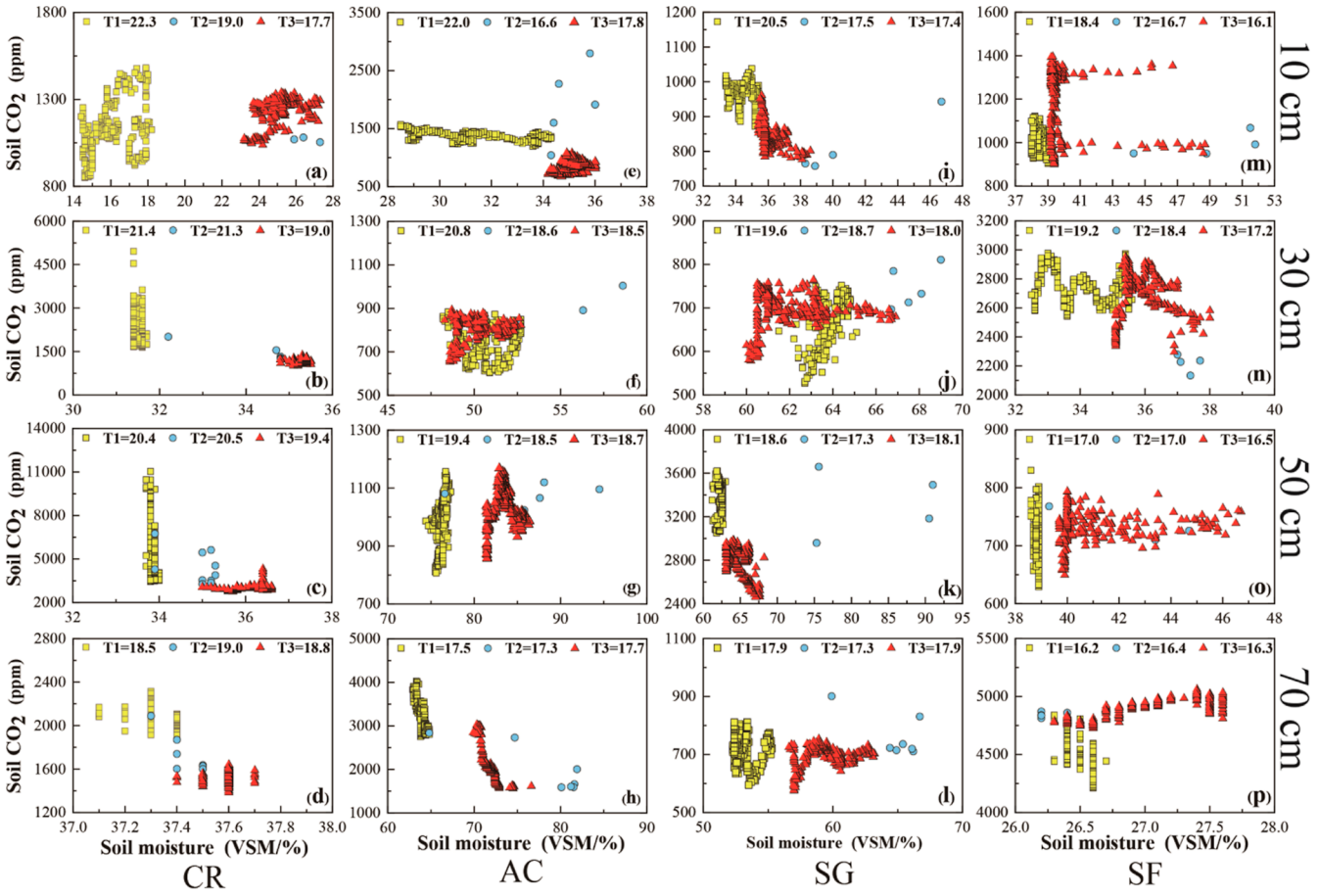

Figure 6. Changes in soil CO_2 and moisture content before, during, and after rainfall under different land uses and the influence of temperature at different times ($T1$, $T2$, and $T3$ represent the average soil temperature content before, during, and after rainfall, respectively).

was primarily affected by meteorological factors and usually reached the highest values in the afternoon. The change in the CO_2 concentration is affected by many factors.[15,46,47] There is a hysteresis between soil temperature and CO_2 concentration, which arises from soil moisture.[48,49] On May 3 and 4, the average daily moisture contents were 39.0 and 38.5%, respectively. The hysteresis time between the temperature and the CO_2 concentration also differed. The hysteresis time was 5 h 15 min on May 3 and 9 h 15 min on May 4. The difference in the soil moisture content in those 2 days was only 0.5%, but the lag time between temperature and CO_2 concentration was approximately double. The difference in the soil moisture content may be one reason for the lag between the temperature and the CO_2 concentration. Due to the lag time between them, there was a negative correlation between the CO_2 concentration and temperature (Figure 5), but other factors may also contribute to the change in soil CO_2, such as soil texture and plant roots. Root exudates can decompose organic matter, thereby modifying the concentration of soil CO_2.[50]

5.3. Effects of the Moisture Content on Soil CO_2. Generally, the soil moisture content will not reach the soil biological wilting point or exceed the field water holding capacity. The small fluctuations in the soil moisture content will not significantly impact the soil CO_2 concentration.[51,52] However, rainfall causes a large variation in the soil moisture content, which ultimately leads to significant changes in the soil CO_2 concentration. During the observation period, the soil moisture content changed significantly, especially during the rainfall period, and the soil moisture increased rapidly in a short time (Figure 6). However, the increase in the soil moisture content varies with different depths, and this difference may be related to the soil permeability coefficient or rainfall.[53] Porosity is one of the factors affecting the soil permeability coefficient. Overall, with the restoration of vegetation, the porosity increases gradually (Table 1), which is beneficial to the infiltration and migration of water. According to the experimental results, there is no significant difference in the change time of the soil moisture content during rainfall, which may be due to the development of extensive cracks in this area, resulting in rapid infiltration of water and reducing the influence of the soil permeability coefficient. Under the influence of rainfall, the soil moisture increased gradually, and soil pores were gradually filled with soil water, reducing the diffusion rate of CO_2 to the atmosphere.

In addition, rainfall can promote microbial activities and strongly stimulate the production of soil CO_2, leading to an increase in the soil CO_2 concentration, which is called the "stimulation effect".[46,55] Previous studies indicated that organic matter and microorganisms can affect the stimulation effect, increasing the release of CO_2 during rainfall.[56] Especially in arid and semiarid regions, the lower water content has limited impacts on microorganism activities. When it rains, the soil water content increases sharply, leading to the rapid utilization of available organic matter preserved in arid environments by

https://doi.org/10.1021/acsearthspacechem.3c00169
ACS Earth Space Chem. 2023, 7, 2062−2072

microorganisms.[57] However, in this study, the CO_2 concentration in most layers showed a significant downward trend when there was a concentrated rainfall (Figure 3). This is likely due to the liveable environments for the survival of microorganisms under such warm and moist environments, and the activities of microorganisms are more active. However, when it rains, microorganisms do not respond quickly to sudden increases in soil water. Another reason is possibly related to the equilibrium process of HCO_3^-, CO_3^{2-}, and CO_2 in soil water.[58] Due to the large porosity and alkalescence of calcareous soil, a large amount of CO_2 is dissolved after rainwater enters the soil pores, which then reacts with carbonate minerals in the soil. As a result, the main form of inorganic C in the water body is HCO_3^-, the concentration of free CO_2 is low, and this chemical process could reduce the concentration of soil CO_2.[59] When rainfall stops, soil water infiltrates rapidly; soil pores are filled with CO_2 gas again, and the CO_2 concentration gradually returns to normal. The downward migration of soil water may cause "pressure" on the soil gas and cause the downward migration of soil gas. As mentioned above, the soil CO_2 concentration increases with increasing depth; therefore, downward migration will reduce the gas concentration in the corresponding layer. Due to the loose structure, with the cessation of rainfall, the downward migration of soil water gradually disappears, and the upward diffusion process of soil air resumes. Because of the shallow soil, there is a transition layer with strong water and gas conductivity between limestone soil and its underlying rocks, and it may also be a channel for soil air diffusion.[39] In addition, the soil moisture increased, and the soil porosity decreased during rainfall. In the case of high moisture, there is an anaerobic environment that is not conducive to the occurrence of soil rhizosphere and microbial respiration,[47,60,61] which may be related to the rapid decrease in the CO_2 concentration in the soil profile during rainfall. Only at a few points did the concentration of soil CO_2 increase, after which it began to decrease, which may be because the sudden increase in moisture stimulated the short-term cycle of soil C. The short-term rapid increase in CO_2 was perhaps caused by the mineralization of organic matter.[55]

When rainfall occurs, the concentration of CO_2 in the soil profile suddenly decreases, accompanied by a rapid increase in the moisture content (Figure 3). After a sudden increase in moisture, the CO_2 concentration would decrease rapidly in a short time, implying that the rapid reduction in CO_2 is related to soil moisture. In the SG profile, the CO_2 concentration before rain was higher than that after rain, except at a depth of 30 cm. At a depth of 30 cm, this performance may be related to the change in soil moisture contents, which were 63.8% before the rain and 62.1% after the rain. This may imply that the high moisture content may inhibit soil respiration,[62,63] and the moisture contents of other layers after rain were higher than those before rain. Previous results of soil CO_2 concentrations and water bodies in this watershed have shown that soil CO_2 decreased rapidly during rainfall, accompanied by a response to the partial pressure of CO_2 in the water bodies at the outlet of the watershed. It was found that both soil CO_2 and rainfall are the main forces driving the epikarst hydrochemical variations.[64] In such a small watershed, the water flow velocity of the underground water outlet was highly sensitive to rainfall and increased quickly.[65,66] Then, the soil solution can quickly enter the river system.[67] In karst areas, the development of pores, especially larger ones, may be able to form a coherent system with groundwater within a short time. In this watershed, the river system was well studied during rainfall,[68] and it was found that the flow and DIC increased rapidly after rainfall, which may be related to the water−rock reaction in the soil system and the rapid decrease in the CO_2 concentration during the rainfall period. However, due to the lack of observation parameters, the specific process cannot be discussed in depth. Unquestionably, in addition to affecting the diffusion rate of soil gas, soil water may also cause dynamics in soil CO_2 due to chemical processes. Thus, in this area, the soil moisture content may play a critical role in the CO_2 dynamics of calcareous soil.

6. CONCLUSIONS

In this study, high-frequency observations of soil CO_2 concentration, temperature, and moisture under rainfall conditions were conducted in soil profiles at different vegetation restoration stages in karst watersheds using online monitoring equipment.

The soil CO_2 concentration showed a bidirectional gradient from top to bottom along the profile; SF and AC had higher CO_2 concentrations, while SG and AC had relatively lower CO_2 concentrations. The soil CO_2 concentration dropped rapidly during rainfall, its amplitude decreased gradually, and the response time decreased greatly with the restoration of vegetation, indicating that the stability of the soil C pool could be improved under the condition of returning farmland to grasslands and forests. The diurnal variation in the CO_2 concentration in several soil profiles obviously changed before and after rainfall. The diurnal variation decreased after rainfall, and the diurnal difference of the four soil profiles decreased. The increasing soil moisture resulted in an increase in the consumption of CO_2 in the soil directly, and high soil moisture decreased the diurnal variation in the soil temperature, which could indirectly weaken the intensity of temperature-related biological processes.

Our study shows that with the restoration of vegetation, the land has a higher capacity for C sequestration, indicating that vegetation restoration could be a significant strategy for the implementation of solid C neutralization. Simultaneously, our research also highlights the necessity of conducting high-frequency in situ observations of special events to further reveal the dynamics of soil C under frequent extreme weather conditions in the future.

AUTHOR INFORMATION

Corresponding Author

Yucong Fu − *State Key Laboratory of Environmental Geochemistry, Institute of Geochemistry, Chinese Academy of Sciences, Guiyang 550081, China; University of Chinese Academy of Sciences, Beijing 100049, China;* orcid.org/0009-0006-5100-5831; Email: fuyucong@mail.gyig.ac.cn

Authors

Jie Zeng − *Key Laboratory of Karst Georesources and Environment (Guizhou University), Ministry of Education, College of Resources and Environmental Engineering, Guizhou University, Guiyang 550025, China*

Zhongjun Wang − *School of Environmental Science and Engineering, Yancheng Institute of Technology, Yancheng 224051, China*

Complete contact information is available at: https://pubs.acs.org/10.1021/acsearthspacechem.3c00169

https://doi.org/10.1021/acsearthspacechem.3c00169
ACS Earth Space Chem. 2023, 7, 2062−2072

Author Contributions

Conceptualization of the study, F.Y.; methodology, F.Y. and W.Z.; writing—original draft preparation, F.Y.; and writing—review and editing, F.Y., J.Z., and W.Z. All authors participated in reviewing and editing the text. All authors have read and agreed to the published version of the manuscript.

Funding

This research was funded by the "National Natural Science Foundation of China" with grant number 42071142 and the "Natural Science Foundation of Shaanxi Province" with grant numbers 2022JZ-19 and 2022JQ-229.

Notes

The authors declare no competing financial interest.

■ ACKNOWLEDGMENTS

The authors thank those at the Puding Karst Ecosystem Research Station for their support of this research.

■ REFERENCES

(1) Friedlingstein, P.; Jones, M. W.; O'Sullivan, M.; Andrew, R. M.; Hauck, J.; Peters, G. P.; Peters, W.; Pongratz, J.; Sitch, S.; Le Quéré, C.; et al. Global carbon budget. *Earth Syst. Sci. Data* **2019**, *11*, 1783−1838.

(2) Kothavala, Z. Extreme precipitation events and the applicability of global climate models to the study of floods and droughts. *Math. Comput. Simul.* **1997**, *43*, 261−268.

(3) Broecker, W. S.; Peng, T. *Greenhouse, Puzzles*, 2nd ed.; Eldigio Press: Palisades, 1998.

(4) Schindler, D. W. The mysterious missing sink. *Nature* **1999**, *398*, 105−107.

(5) Schimel, D. S. Terrestrial ecosystems and the carbon cycle. *Global Change Biol.* **2010**, *1*, 77−91.

(6) Melillo, J. M.; Steudler, P. A.; Aber, J. D.; Newkirk, K.; Lux, H.; Bowles, F. P.; Catricala, C.; Magill, A.; Ahrens, T.; Morrisseau, S. Soil warming and carbon-cycle feedbacks to the climate system. *Science* **2002**, *298*, 2173−2176.

(7) Ojanen, P.; Minkkinen, K.; Alm, J.; Penttilä, T. Soil-atmosphere CO_2, CH_4 and N_2O fluxes in boreal forestry-drained peatlands. *For. Ecol. Manage.* **2010**, *260*, 411−421.

(8) Wu, X.; Yao, Z. N. B.; Brüggemann, N.; Shen, Z.; Wolf, B.; Dannenmann, M.; Zheng, X.; Butterbach-Bahl, K. Effects of soil moisture and temperature on CO_2 and CH_4 soil-atmosphere exchange of various land use/cover types in a semi-arid grassland in Inner Mongolia, China. *Soil Biol. Biochem.* **2010**, *42*, 773−787.

(9) Hatfield, J. L.; Prueger, J. H. Agroecology: Implications for Plant Response to Climate Change. In *Crop Adaptation to Climate Change*; Wiley, 2011; pp 27−43.

(10) Ma, J.; Wang, Z.; Stevenson, B.; Zheng, X.; Li, Y. An inorganic CO_2 diffusion and dissolution process explains negative CO_2 fluxes in saline/alkaline soils. *Sci. Rep.* **2013**, *3*, 2025.

(11) O'Sullivan, M.; Gravatt, M.; Popineau, J.; O'Sullivan, J.; Mannington, W.; McDowell, J. Carbon dioxide emissions from geothermal power plants. *Renewable Energy* **2021**, *175*, 990−1000.

(12) Liu, Z.; Dreybrodt, W.; Wang, H. A new direction in effective accounting for the atmospheric CO_2 budget: Considering the combined action of carbonate dissolution, the global water cycle and photosynthetic uptake of DIC by aquatic organisms. *Earth-Sci. Rev.* **2010**, *99*, 162−172.

(13) Flechard, C.; Neftel, A.; Jocher, M.; Ammann, C.; Leifeld, J.; Fuhrer, J. Temporal changes in soil pore space CO_2 concentration and storage under permanent grassland. *Agric. For. Meteorol.* **2007**, *142*, 66−84.

(14) Tang, J.; Baldocchi, D.; Qi, Y.; Xu, L. Assessing soil CO_2 efflux using continuous measurements of CO_2 profiles in soils with small solid-state sensors. *Agric. For. Meteorol.* **2003**, *118*, 207−220.

(15) Jassal, R.; Black, A.; Novak, M.; Morgenstern, K.; Nesic, Z.; Gaumont-Guay, D. Relationship between soil CO_2 concentrations and forest-floor CO_2 effluxes. *Agric. For. Meteorol.* **2005**, *130*, 176−192.

(16) Huang, L.; Zhang, Z.; Li, X. Soil CO_2 concentration in biological soil crusts and its driving factors in a revegetated area of the Tengger Desert, Northern China. *Environ. Earth Sci.* **2014**, *72*, 767−777.

(17) Ryan, M.; Law, B. Interpreting, measuring, and modeling soil respiration. *Biogeochemistry* **2005**, *73*, 3−27.

(18) Chamizo, S.; Rodríguez-Caballero, E.; Sánchez-Cañete, E. P.; Domingo, F.; Cantón, Y. Temporal dynamics of dryland soil CO_2 efflux using high-frequency measurements: Patterns and dominant drivers among biocrust types, vegetation and bare soil. *Geoderma* **2022**, *405*, 115404.

(19) Maier, M.; Schack-Kirchner, H.; Hildebrand, E.; Schindler, D. Soil CO_2 efflux vs. soil respiration: Implications for flux models. *Agric. For. Meteorol.* **2011**, *151*, 1723−1730.

(20) Johnson, M. S.; Lehmann, J.; Riha, S.; Krusche, A. V.; Richey, J. E.; Ometto, J. P.; Couto, E. CO_2 efflux from Amazonian headwater streams represents a significant fate for deep soil respiration. *Geophys. Res. Lett.* **2008**, *35*, L17401.

(21) Hotchkiss, E.; Hall, R. O., Jr.; Sponseller, R.; Butman, D.; Klaminder, J.; Laudon, H.; Rosvall, M.; Karlsson, J. Sources of and processes controlling CO_2 emissions change with the size of streams and rivers. *Nat. Geosci.* **2015**, *8*, 696−699.

(22) Winterdahl, M.; Wallin, M.; Karlsen, R.; Laudon, H.; Öquist, M.; Lyon, S. Decoupling of carbon dioxide and dissolved organic carbon in boreal headwater streams. *J. Geophys. Res.: Biogeosci.* **2016**, *121*, 2630−2651.

(23) Zhou, G.; Huang, J.; Tao, X.; Luo, Q.; Zhang, R.; Liu, Z. Overview of 30 years of research on solubility trapping in Chinese karst. *Earth-Sci. Rev.* **2015**, *146*, 183−194.

(24) Song, X.; Gao, Y.; Wen, X.; Guo, D.; Yu, G.; He, N.; Zhang, J. Carbon sequestration potential and its eco-service function in the karst area, China. *J. Geogr. Sci.* **2017**, *27*, 967−980.

(25) Hirano, T.; Kim, H.; Tanaka, Y. Long-term half-hourly measurement of soil CO_2 concentration and soil respiration in a temperate deciduous forest. *J. Geophys. Res.: Atmos.* **2003**, *108* (D20), 4631.

(26) Moya, M. R.; Sánchez-Cañete, E. P.; Vargas, R.; López-Ballesteros, A.; Oyonarte, C.; Kowalski, A. S.; Serrano-Ortiz, P.; Domingo, F. CO_2 Dynamics Are Strongly Influenced by Low Frequency Atmospheric Pressure Changes in Semiarid Grasslands. *J. Geophys. Res.: Biogeosci.* **2019**, *124*, 902−917.

(27) Spohn, M.; Holzheu, S. Temperature controls diel oscillation of the CO_2 concentration in a desert soil. *J. Geophys. Res.: Biogeosci.* **2021**, *156*, 279−292.

(28) Rey, A. Mind the gap: non-biological processes contributing to soil CO_2 efflux. *Global Change Biol.* **2015**, *21*, 1752−1761.

(29) Wang, Z.; Yue, F.; Lu, J.; Wang, Y.; Qin, C.; Ding, H.; Xue, L.; Li, S. New insight into the response and transport of nitrate in karst groundwater to rainfall events. *Sci. Total Environ.* **2022**, *818*, 151727.

(30) Qin, C.; Li, S.; Yu, G.; Bass, A.; Yue, F.; Xu, S. Vertical variations of soil carbon under different land uses in a karst critical zone observatory (CZO), SW China. *Geoderma* **2022**, *412*, 115741.

(31) Wang, Z.; Yue, F.; Xue, L.; Wang, Y.; Qin, C.; Zeng, J.; Ding, H.; Fu, Y.; Li, S. Soil nitrogen transformation in different land use and implications for karst soil nitrogen loss controlling. *Catena* **2023**, *225*, 107026.

(32) Chen, X.; Zhang, Z.; Soulsby, C.; Cheng, Q.; Binley, A.; Jiang, R.; Tao, M. Characterizing the heterogeneity of karst critical zone and its hydrological function: an integrated approach. *Hydrol. Processes* **2018**, *32*, 2932−2946.

(33) Zhao, M.; Zeng, C.; Liu, Z.; Wang, S. Effect of different land use/land cover on karst hydrogeochemistry: A paired catchment study of Chenqi and Dengzhanhe, Puding, Guizhou, SW China. *J. Hydrol.* **2010**, *388*, 121−130.

(34) Hari, P.; Pumpanen, J.; Huotari, J.; Kolari, P.; Grace, J.; Vesala, T.; Ojala, A. High frequency measurements of productivity of

planktonic algae using rugged nondispersive infrared carbon dioxide probes. *Limnol. Oceanogr.: Methods* **2008**, *6*, 347−354.
(35) Pumpanen, J.; Ilvesniemi, H.; Peramaki, M.; Hari, P. Seasonal patterns of soil CO_2 efflux and soil CO_2 concentration in a Scots pine forest. *Global Change Biol.* **2003**, *9*, 371−382.
(36) Xu, S.; He, S. The CO_2 regime in soil profile and its drive to dissolution in carbonate rock area. *Cardiol. Sin.* **1996**, *15*, 50−57.
(37) Benavente, J.; Vadillo, I.; Carrasco, F.; Soler, A.; Liñán, C.; Moral, F. Air Carbon Dioxide Contents in the Vadose Zone of a Mediterranean Karst. *Vadose Zone J.* **2010**, *9*, 126−136.
(38) Liu, F.; Liu, C.; Wang, S.; Lü, Y. Temporal and spatial variations of greenhouse gases concentrations in soils in karst stone desertification areas in central part of Guizhou Province. *Environ. Sci.* **2009**, *30*, 3136−3141.
(39) Tsypin, M.; Macpherson, G. The effect of precipitation events on inorganic carbon in soil and shallow groundwater, Konza Prairie LTER Site, NE Kansas, USA. *Appl. Geochem.* **2012**, *27*, 2356−2369.
(40) Austin, A. T.; Mendez, M. S.; Ballare, C. L. Photodegradation alleviates the lignin bottleneck for carbon turnover in terrestrial ecosystems. *Proc. Natl. Acad. Sci. U.S.A.* **2016**, *113*, 4392−4397.
(41) Bouma, T. J.; Nielsen, K. L.; Eissenstat, D. M.; Lynch, J. P. Estimating respiration of roots in soil: interactions with soil CO2, soil temperature and soil water content. *Plant Soil* **1997**, *195*, 221−232.
(42) Han, G.; Luo, Y.; Li, D.; Xia, J.; Xing, Q.; Yu, J. Ecosystem photosynthesis regulates soil respiration on a diurnal scale with a short-term time lag in a coastal wetland. *Soil Biol. Biochem.* **2014**, *68*, 85−94.
(43) De Gregorio, S.; Camarda, M.; Longo, M.; Cappuzzo, S.; Giudice, G.; Gurrieri, S. Long-term continuous monitoring of the dissolved CO_2 performed by using a new device in groundwater of the Mt. Etna (southern Italy). *Water Res.* **2011**, *45*, 3005−3011.
(44) Huang, Y.; Hung, C.; Lin, I.; Kume, T.; Menyailo, O.; Cheng, C. Soil respiration patterns and rates at three Taiwanese forest plantations: dependence on elevation, temperature, precipitation, and litterfall. *Bot. Stud.* **2017**, *58*, 49.
(45) Cao, M.; Jiang, Y.; Chen, Y.; Fan, J.; He, Q. Variations of soil CO_2 concentration and pCO_2 in a cave stream on different time scales in subtropical climatic regime. *Catena* **2020**, *185*, 104280.
(46) Jones, D.; Murphy, D. Microbial response time to sugar and amino acid additions to soil. *Soil Biol. Biochem.* **2007**, *39*, 2178−2182.
(47) Mcnicol, G.; Silver, W. Separate effects of flooding and anaerobiosis on soil greenhouse gas emissions and redox sensitive biogeochemistry. *J. Geophys. Res.: Biogeosci.* **2014**, *119*, 557−566.
(48) Riveros-Iregui, D. A.; Emanuel, R. E.; Muth, D. J.; McGlynn, B. L.; Epstein, H. E.; Welsch, D. L.; Wraith, J. M. Diurnal hysteresis between soil CO_2 and soil temperature is controlled by soil water content. *Geophys. Res. Lett.* **2007**, *34*, 17.
(49) Zhang, Q.; Katul, G.; Oren, R.; Daly, E.; Manzoni, S.; Yang, D. The hysteresis response of soil CO_2 concentration and soil respiration to soil temperature. *J. Geophys. Res.: Biogeosci.* **2015**, *120*, 1605−1618.
(50) Paterson, E.; Hall, J. M.; Rattray, E. A. S.; Griffiths, B. S.; Ritz, K.; Killham, K. Effect of elevated CO_2 on rhizosphere carbon flow and soil microbial processes. *Global Change Biol.* **1997**, *3*, 363−377.
(51) Fang, C.; Moncrieff, J. B. The dependence of soil CO_2 efflux on temperature. *Soil Biol. Biochem.* **2001**, *33*, 155−165.
(52) Kiefer, R. Soil carbon dioxide concentrations and climate in a humid subtropical environmen. *Prof. Geogr.* **1990**, *42*, 182−194.
(53) Issazadeh, L.; Ismail Umar, M.; Al-Sulaivany, S. I. A.; Hassanpour, J. Geostatistical Analysis of the Permeability Coefficient in Different Soil Textures. *Contemp. Agric.* **2018**, *67*, 119−124.
(54) Yi, R.; Xu, X.; Zhang, Y.; Ye, Z.; Wang, K. Grain for Green Project May Not Threaten Ecosystem Sustainability by Degrading Water Availability in Humid Karst Landscapes. *Water Resour. Res.* **2023**, *59*, No. e2022WR032415.
(55) Fierer, N.; Schimel, J. A proposed mechanism for the pulse in carbon dioxide production commonly observed following the rapid rewetting of a dry soil. *Soil Sci. Soc. Am. J.* **2003**, *67*, 798−805.
(56) Jiang, Z.; Bian, H.; Xu, L.; Li, M.; He, N. Pulse effect of precipitation: Spatial patterns and mechanisms of soil carbon emissions. *Front. Ecol. Evol.* **2021**, *9*, 673310.
(57) Xu, L.; Baldocchi, D. D.; Tang, J. How soil moisture, rain pulses, and growth alter the response of ecosystem respiration to temperature. *Global Biogeochem. Cycles* **2004**, *18*, GB4002.
(58) Lambin, E.; Turner, B.; Geist, H.; Agbola, S.; Angelsen, A.; Bruce, J.; Coomes, O.; Dirzo, R.; Fischer, G.; Folke, C.; et al. The causes of land-use and land-cover change: moving beyond the myths. *Glob. Environ. Change* **2001**, *11*, 261−269.
(59) Zhong, J.; Li, S.; Tao, F.; Yue, F.; Liu, C. Sensitivity of chemical weathering and dissolved carbon dynamics to hydrological conditions in a typical karst river. *Sci. Rep.* **2017**, *7*, 42944.
(60) Jimenez, K.; Starr, G.; Staudhammer, C.; Schedlbauer, J.; Loescher, H.; Malone, S.; Oberbauer, S. Carbon dioxide exchange rates from short-and long-hydroperiod Everglades freshwater marsh. *J. Geophys. Res.: Biogeosci.* **2012**, *117*, G4.
(61) Vidon, P.; Marchese, S.; Welsh, M.; McMillan, S. Impact of precipitation intensity and riparian geomorphic characteristics on greenhouse gas emissions at the soil-atmosphere interface in a water-limited riparian zone. *Water, Air, Soil Pollut.* **2016**, *227*, 8.
(62) Liu, Y.; Wan, K.; Tao, Y.; Li, Z.; Zhang, G.; Li, S.; Chen, F. Carbon dioxide flux from rice paddy soils in central China: effects of intermittent flooding and draining cycles. *PLoS One* **2013**, *8*, No. e56562.
(63) Gabriel, C.; Kellman, L. Investigating the role of moisture as an environmental constraint in the decomposition of shallow and deep mineral soil organic matter of a temperate coniferous soil. *Soil Biol. Biochem.* **2014**, *68*, 373−384.
(64) Yang, R.; Liu, Z.; Zeng, C.; Zhao, M. Response of epikarst hydrochemical changes to soil CO_2 and weather conditions at Chenqi, Puding, SW China. *J. Hydrol.* **2012**, *468−469*, 151−158.
(65) Zhang, Z.; Chen, X.; Chen, X.; Shi, P. Quantifying time lag of epikarst-spring hydrograph response to rainfall using correlation and spectral analyses. *Hydrogeol. J.* **2013**, *21*, 1619−1631.
(66) Liu, Z.; Li, Q.; Sun, H.; Wang, J. Seasonal, diurnal and storm-scale hydrochemical variations of typical epikarst springs in subtropical karst areas of SW China: soil CO_2 and dilution effects. *J. Hydrol.* **2007**, *337*, 207−223.
(67) Liu, L.; Wang, D.; Huang, H.; Xu, G. Use of Hydrologic Time Series Data for Analysis the Karstic Drought Characteristic. *Appl. Mech. Mater.* **2014**, *641−642*, 127−131.
(68) Qin, C.; Li, S.; Waldron, S.; Yue, F.; Wang, Z.; Zhong, J.; Ding, H.; Liu, C. High-frequency monitoring reveals how hydrochemistry and dissolved carbon respond to rainstorms at a karstic critical zone, Southwestern China. *Sci. Total Environ.* **2020**, *714*, 136833.

https://doi.org/10.1021/acsearthspacechem.3c00169
ACS Earth Space Chem. 2023, 7, 2062−2072